Quantum walks and trapping on regular hyperbranched fractals

2009 J. Phys. A: Math. Theor. 42 225003

(http://iopscience.iop.org/1751-8121/42/22/225003)

IOP PUBLISHING JOURNAL OF PHYSICS A: MATHEMATICAL AND THEORETICAL

J. Phys. A: Math. Theor. **42** (2009) 225003 (10pp) doi:10.1088/1751-8113/42/22/225003

Quantum walks and trapping on regular hyperbranched fractals

Antonio Volta

[1] Theoretische Polymerphysik, Universität Freiburg, Hermann-Herder-Straße 3, D-79104 Freiburg, Germany
[2] Dipartimento di Colture Arboree, University of Bologna, viale Fanin 46, I-40127 Bologna, Italy

E-mail: antonio.volta@unibo.it

Received 19 January 2009, in final form 8 April 2009
Published 14 May 2009
Online at stacks.iop.org/JPhysA/42/225003

Abstract

The present work studies the behaviour of continuous time quantum walks on regular hyperbranched fractals, whose centre is a trap. We focus on the variations of the eigenvalue spectrum of the transfer operator by tuning the trap strength from zero to infinity. We show that the degenerate eigenvalues are independent from the trap strength and can be obtained analytically. Due to this the mean survival probability is just in the intermediate range affected by the trap strength; moreover, because of the presence of real eigenvalues, the asymptotical probability of being outside the trap is not zero.

PACS numbers: 05.60.Gg, 05.40.−a

(Some figures in this article are in colour only in the electronic version)

1. Introduction

The trapping problem is a fundamental and long-standing topic in many fields of science ranging from physics to biology, plant physiology, etc, ... Recent studies applied this problem to quantum networks for phenomena where coherent dynamical processes are involved such as ultracold Rydberg gases [1, 2] as well as photosynthetic processes [3–5]. The coherent exciton transfer is well described by the quantum-mechanical version of random walks, the so-called quantum walks [6–8]. There are two kinds of quantum walks: the walks which occur at discrete time steps and the continuous time quantum walks (CTQWs). In this work, CTQWs are applied to regular hyperbranched fractals (RHFs) with a central trap to simulate fractal harvesting dynamics. We focus on the relationship between the eigenvalue spectrum of the transfer operator and the trap strength γ. The value of γ only partially affects the spectrum. The meaning of this property becomes clear calculating, e.g., the mean survival probability [1, 9]. The paper is so structured: in section 2 one recalls the basis of CTQWs, while in

section 3 is given a description of the RHFs. Section 4 analyses the eigenvalue spectrum of the transfer operator developing the problem in three steps: $\gamma = 0, 0 < \gamma < \infty$ and $\gamma \to \infty$. The consequences of the different spectra are then shown in section 5 by calculating the mean survival probability. In section 6 a possible application to photosynthetic complexes is proposed. Finally in section 7 the conclusion is provided.

2. Continuous time quantum walks

In this section we provide an overview of the continuous time quantum walks. This mathematical tool is used to describe coherent quantum–mechanical transport. Let us start introducing (classical) continuous time random walks (CTRWs). The CTRWs are described by the master equation [10–12]

$$\frac{\mathrm{d}}{\mathrm{d}t} p_{\boldsymbol{k},\boldsymbol{j}}(t) = \sum_{l} T_{kl}\, p_{l,\boldsymbol{j}}(t), \tag{1}$$

where $p_{\boldsymbol{k},\boldsymbol{j}}(t)$ is the conditional probability to find the walker at time t at node $\boldsymbol{k}$ being $p_{\boldsymbol{k},\boldsymbol{j}}(0) = \delta_{kj}$ and $\mathbf{T} = (T_{kl})$ the transfer operator. For unbiased CTRWs without traps, one has equal rates to transfer from one node to one of the nearest neighbours, set for simplicity in the following equal to 1. Under these assumptions, the transfer operator $\mathbf{T_0} = (T_{0kj})$ is reduced to the simple form $\mathbf{T_0} = -\mathbf{A_0}$, where $\mathbf{A_0}$ is the discrete form of the Laplacian operator, i.e., the so-called connectivity matrix [13]. $\mathbf{A_0}$ is such that its off-diagonal elements A_{ij} are -1 if $\boldsymbol{i}$ and $\boldsymbol{j}$ are connected and 0 otherwise (note that in modulus they are the same of the adjacency matrix [14]). The diagonal elements are $A_{0ii} = -\sum_{j=1}^{\prime N} A_{0ij}$ where the prime excludes the case $j = i$ from the sum. Hence $\mathbf{A_0}$ results a real symmetric matrix.

The passage to CTQWs is done by identifying the transfer operator with the Hamiltonian of the system, i.e., $\mathbf{H_0} = -\mathbf{T_0}$, see [7, 15, 16]. As remarked in [15] this is not the only way to define CTQWs. In fact, for certain graphs there is some freedom in defining the diagonal elements of the Hamiltonian. Moreover for regular networks, i.e., for networks where all nodes have the same functionality or degree [17], the same quantum dynamics is obtained by different choices of Hamiltonian which anyhow must be a unitary operator. The idea is that we have N orthonormal $|\boldsymbol{j}\rangle$ states localized at each corresponding node, that form a basis set which cover the whole accessible Hilbert space, i.e., $\langle \boldsymbol{k}|\boldsymbol{j}\rangle = \delta_{kj}$ and $\sum_j |\boldsymbol{j}\rangle\langle \boldsymbol{j}| = \mathbf{1}$, with $\mathbf{1}$ being the identity operator. The transition amplitude from the initial state $|\boldsymbol{j}\rangle$ to state $|\boldsymbol{k}\rangle$ obeys the Schrödinger equation (for simplicity we set $\hbar \equiv 1$)

$$\mathrm{i}\frac{\mathrm{d}}{\mathrm{d}t}\alpha_{\boldsymbol{k},\boldsymbol{j}}(t) = \sum_{l} H_{kl}\alpha_{l,\boldsymbol{j}}(t), \tag{2}$$

which gives rise to the formal solution

$$\alpha_{\boldsymbol{k},\boldsymbol{j}}(t) = \langle \boldsymbol{k}|\exp(-\mathrm{i}\mathbf{H}t)|\boldsymbol{j}\rangle. \tag{3}$$

The transition probability is given by the square of $\alpha_{\boldsymbol{k},\boldsymbol{j}}(t)$, i.e., $\pi_{\boldsymbol{k},\boldsymbol{j}}(t) = |\alpha_{\boldsymbol{k},\boldsymbol{j}}(t)|^2$. Although there exists a formal similarity between CTWRs and CTQWs, quantum mechanically it holds $\sum_k \pi^2_{\boldsymbol{k},\boldsymbol{j}}(t) = 1$ instead of $\sum_k p_{\boldsymbol{k},\boldsymbol{j}}(t) = 1$, see also [18].

3. The structure

Regular hyperbranched fractals (RHFs) [9] of generation $g = 3$ and functionality $f = 3, 4$ are displayed in figure 1. The RHFs with functionality $f = 4$ are known also as Vicsek fractals [19]. To build these kind of structures one takes the object of generation $g = 1$, i.e.,

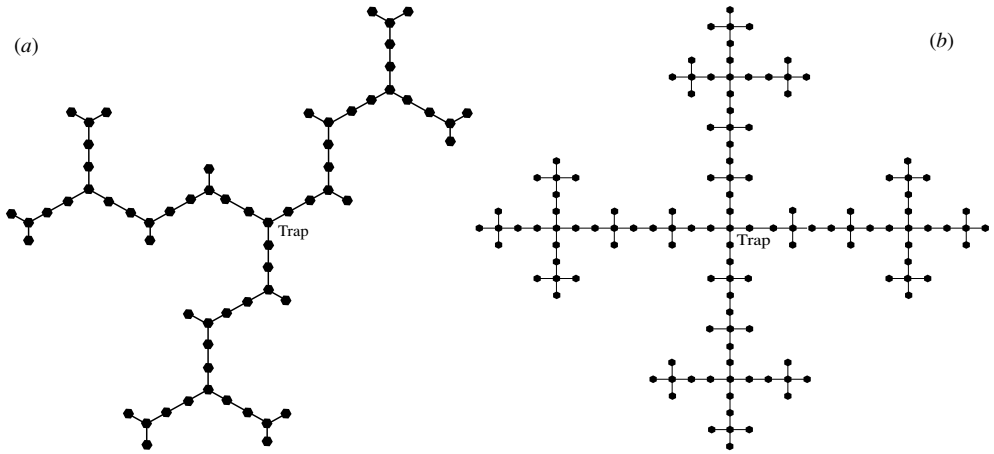

Figure 1. Regular hyperbranched fractals of generation $g = 3$ for functionality $f = 3$ (a) and functionality $f = 4$ (b). The central node of the structure is the trap site.

a star structure with the core connected through f branches to f external nodes. The next generation $g = 2$ is obtained by binding to the external nodes f identical copies of itself through f bonds; we get so a new starwise pattern of $(f + 1)^2$ nodes, see [13, 20] for more details. The same procedure is repeated until to reach the required size of $(f + 1)^g$ sites. The fractal dimension depends on the functionality f as follows:

$$\bar{d}_r = \frac{\ln(f + 1)}{\ln 3}. \tag{4}$$

4. Evaluation of the T spectrum

The spectrum of **T** is responsible for many dynamic properties for both classical networks and quantum networks [21–23]. We analyse the eigenvalue spectrum of RHFs in three different steps in order to underline the special behaviour when $\gamma = 0$ and $\gamma \to \infty$.

4.1. RHFs without trap

We first consider the unperturbed case, i.e., when **H** is equal to $\mathbf{H_0}$. We report here an algebraic iterative procedure found by Blumen *et al* in [13, 20], which reduces the general eigenvalue problem to the solution of cubic equations. This is due to the fact that the RHFs rescale under a real space renormalization transformation, see [20, 24] for details. Knowing the eigenvalues of the RHFs at generation g one obtains the eigenvalues of generation $g + 1$ through

$$P\left(\lambda_i^{(g+1)}\right) = \lambda_i^g, \tag{5}$$

where $P(\lambda)$ is the polynomial

$$P(\lambda) = \lambda(\lambda - 3)(\lambda - f - 1). \tag{6}$$

We set $P(\lambda) = a$ and equation (6) is recombined so that it reads

$$\lambda^3 - (f + 4)\lambda^2 + 3(f + 1)\lambda - a = 0. \tag{7}$$

Introducing

$$p = \tfrac{1}{3}\left[f(f-1)+7\right], \tag{8}$$

$$q = \tfrac{1}{27}(5-f)(f+4)(2f-1) \tag{9}$$

and

$$\rho = |p/3|^{3/2}, \tag{10}$$

the roots of equation (6) are given by the Cardano solutions

$$\lambda_\nu = (f+4)/7 + 2\rho^{1/3}\cos[(\phi + 2\pi\nu)/3)] \qquad \text{with} \qquad \nu \in \{1,2,3\}. \tag{11}$$

Except $\lambda_i = 0$, each eigenvalue of generation g gives rise to three new eigenvalues. The non-degenerate eigenvalues include $\lambda = 0, \lambda = (f+1)$ and other eigenvalues generated by the 'seed' $\lambda = (f+1)$. This means that for example, at the second generation of the fractal, we have five non-degenerate eigenvalues, i.e., the above-mentioned $\lambda = 0, \lambda = (f+1)$ and the three 1's obtained by substituting $a = (f+1)$ into equation (7). The degeneracy of the degenerate eigenvalues depends on the generation where they appeared for the first time; $\lambda = 1$ results the most present with occurrence given by

$$\Delta_g = (f-2)(f+1)^{g-1} + 1. \tag{12}$$

4.2. RHFs with central trap

Let us put a trap in the centre of the network (node **1**) by following an approach based on perturbation theory [1, 25–27]. In mathematical terms, we deal with a new Hamiltonian $\mathbf{H} = \mathbf{H_0} + \mathrm{i}\mathbf{\Gamma}$, where $\Gamma_{mn} = \gamma\delta_{1m}\delta_{1n}$. $\mathbf{H}$ is a complex symmetric matrix, therefore, if the matrix is diagonalizable, we have an orthonormal set of eigenvectors [28] as in the real case. The eigenvalue spectrum of $\mathbf{H}$ presents, as in the unperturbed case, degenerate and non-degenerate eigenvalues. Because of the non-Hermiticity of the operator, in general we get N complex eigenvalues $\lambda_l = \epsilon_l - \mathrm{i}\gamma_l$. The diagonalization of $\mathbf{H}$ up to $g = 5$ was computed using the Fortran the routine RS of the EISPACK package [29] for $\gamma = 0$ and the routine CS see [30] otherwise. The strength of γ was varied throughout the range $0 < \gamma < \infty$. What we found out is that only the non-degenerate eigenvalues depend on γ. This means that the degenerate eigenvalues are the same of $\mathbf{H_0}$, so that they can be calculated as in section (4.1). Such a property results clear looking at the eigenvectors. In fact following the idea of Jayanthi and Wu in [19] the eigenvectors with central displacement equal to 0 give rise to degenerate modes. In our case if the first component of the eigenvector is 0, then the imaginary operator $\mathbf{\Gamma}$ is not involved in the calculation of the eigenvalues. Now we can also easily see why the matrices associated with perturbed RHFs are always diagonalizable. A complex symmetric matrix is not diagonalizable if we have at least one isotropic eigenvector, i.e., a self-orthogonal vector z, which satisfies the relationship $zz^T = 0$. An isotropic eigenvector can be associated only with eigenspaces of dimension larger than one [31]. The possibility to have an isotropic eigenvector is excluded because the degenerate eigenvalues depend only on $\mathbf{A}_0$, which is a *real* symmetric matrix, whose eigenvectors do not fulfil the self-orthogonality condition.

We split the analysis of what happens into the imaginary part and the real part of the eigenvalues. To assist the reader, in the next three figures each eigenvalue is always associated with the same colour in all plots. Figure 2 shows

$$\frac{\gamma_i}{\sum_l \gamma_l} = \frac{\gamma_i}{Tr(\mathbf{\Gamma})} = \frac{\gamma_i}{\gamma} \leqslant 1, \tag{13}$$

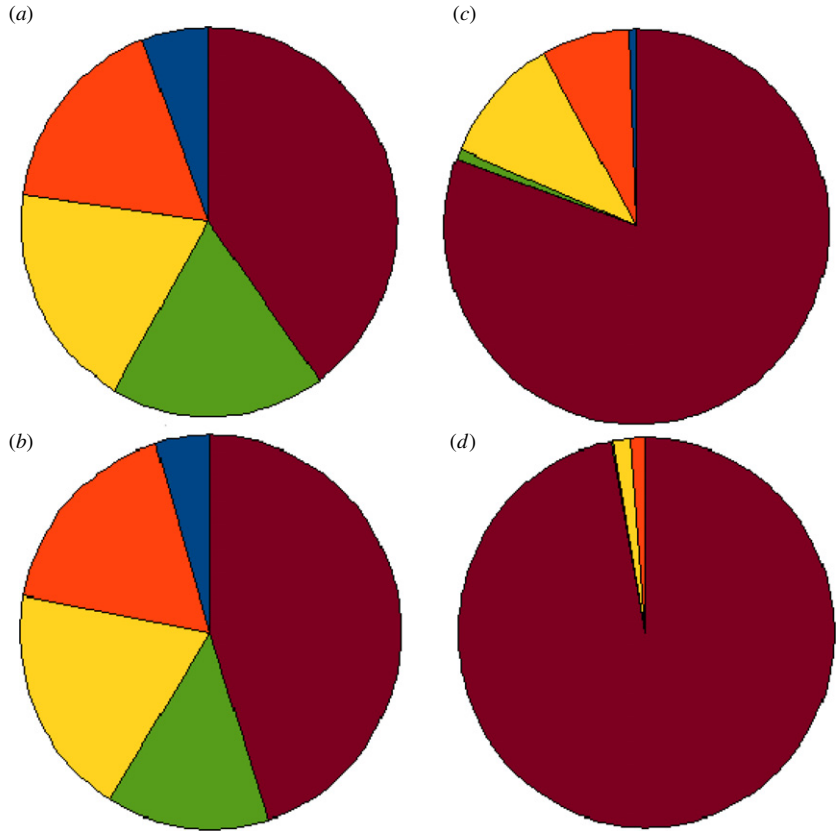

Figure 2. Contributions of the ratios γ_l/γ for RHFs of generation 2 and functionality 3 with different trap strengths. Cake plot (*a*): $\gamma = 0.5$, $\lambda_{\text{purple}} = 4.5138 + \text{i}0.2000$ and $\gamma_{\text{purple}}/\gamma = 40\%$. Cake plot (*b*): $\gamma = 1$, $\lambda_{\text{purple}} = 4.3519 + \text{i}0.4506$ and $\gamma_{\text{purple}}/\gamma = 45\%$. Cake plot (*c*): $\gamma = 4$, $\lambda_{\text{purple}} = 3.2606 + \text{i}3.2250$ and $\gamma_{\text{purple}}/\gamma = 81\%$. Cake plot (*d*): $\gamma = 10$, $\lambda_{\text{purple}} = 3.0316 + \text{i}9.6971$ and $\gamma_{\text{purple}}/\gamma = 97\%$.

for RHFs of generation $g = 2$ and functionality $f = 3$ for $\gamma = 0.5$ (a), $\gamma = 1$ (b), $\gamma = 4$ (c) and $\gamma = 10$ (d). Just the five non-degenerate eigenvalues contribute as expected. Let us call the eigenvalue with the biggest imaginary part $\lambda_{\text{purple}} = \epsilon_{\text{purple}} + \text{i}\gamma_{\text{purple}}$ corresponding to the purple portion of the cake plots of figure 2. The bigger γ, the more concentrated contribution in just γ_{purple}. Thus the relationship $\gamma_{\text{purple}}/\gamma \lesssim 1$ holds for big γ, see figure 2(*d*). In figure 3 the behaviour of γ_l of non-degenerate eigenvalues is shown except γ_{purple}. As we can see all four curves reach a maximum for γ between 0.8 and 4 and then start to decrease. This behaviour will appear important to understand the basic result of section 5. In figure 4, the real part of the eigenvalues ϵ_l is plotted versus γ for RHFs of generation $g = 2$ and functionality $f = 3$. The constant dashed red lines are associated with degenerate eigenvalues that confirm its independence from γ. The solid lines represent the behaviour of the ϵ_l associated with non-degenerate eigenvalues. We note a convergence of four of these to the dashed lines when γ increases. Only ϵ_{purple} has negative derivative and decreases from $\epsilon_{\text{purple}} = \max_{\epsilon_l} \epsilon_l$ to $\epsilon_{\text{purple}} = f$. We chose to plot referred to RHFs of low functionality and low generation in order to make clearer the phenomenon. Anyhow we noted numerically similar behaviour up to generation $g = 5$ for functionalities $f = 3, 4$.

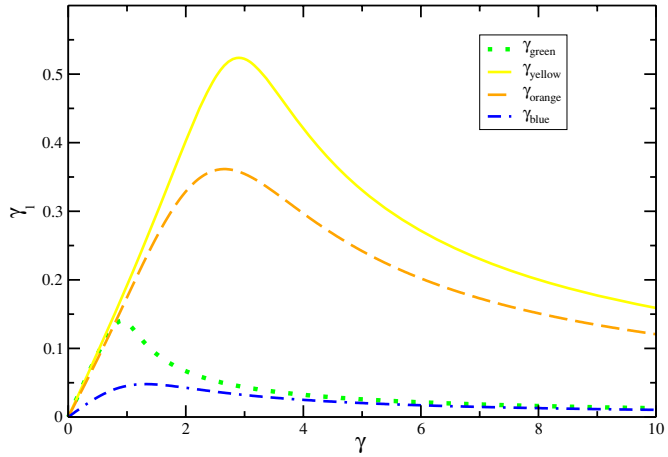

Figure 3. γ_l versus γ for RHFs of $f = 3$ and $g = 2$. The four functions show the behaviour of the non-degenerate eigenvalues except γ_{purple}. The colours help to associate γ_l of this figure with γ_l of the same colour of figure 2.

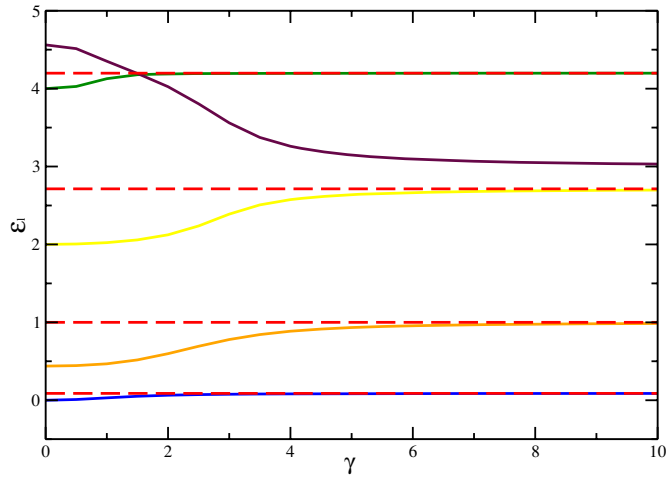

Figure 4. ϵ_l versus γ for RHFs of $f = 3$ and $g = 2$. The purple, yellow, orange, green and blue solid lines represent ϵ_l corresponding to γ_l of figure 2. The red dashed lines represent the degenerate eigenvalues constant with respect to γ.

4.3. Limiting case: $\gamma \to \infty$

If γ tends to infinity, then λ_{purple} assumes the value $\lambda_{\text{purple}} = f + \mathrm{i}\gamma$ while the other eigenvalues assume a real asymptotic value equal to one of the already known degenerate eigenvalues. Apart from the unique remaining imaginary eigenvalue, we will get for each eigenvalue a degeneracy multiple of f, like in [9]. This can be easily demonstrated for RHFs of first generation. In fact it can be shown that the characteristic polynomial of **H** associated with an RHF with functionality f looks

$$(1-\lambda)^{f-2}(\lambda^2 - (1+f+\mathrm{i}\gamma)\lambda + \mathrm{i}\gamma) = 0. \tag{14}$$

The roots of equation (14) are $\lambda = 1$, $(f-2)$-times degenerated and

$$\lambda_{+-} = \frac{1+f+\mathrm{i}\gamma \pm \sqrt{-\gamma^2+2\mathrm{i}\gamma(f-1)+(f-1)^2+4f}}{2}. \tag{15}$$

Inside the square root of equation (15) we can neglect $4f \ll \gamma^2$ and it becomes straightforward

$$\lambda_{+-} \simeq \frac{1+f+\mathrm{i}\gamma \pm \sqrt{[\mathrm{i}\gamma+(f-1)]^2}}{2} = \frac{1+f+\mathrm{i}\gamma \pm [\mathrm{i}\gamma+(f-1)]}{2} = \begin{cases} f+\mathrm{i}\gamma \\ 1. \end{cases} \tag{16}$$

In summary for the first generation, when $\gamma \to \infty$ the eigenvalue 1 appears $(f-1)$-times and $f+\mathrm{i}\gamma$ once.

5. Mean survival probability

The ideal experiment would be performed by exciting exactly one node $\boldsymbol{j} \neq \mathbf{1}$ at time $t = 0$ and to monitor the probability $\pi_{\boldsymbol{k},\boldsymbol{j}}(t)$ to be at node $\boldsymbol{k} \neq \mathbf{1}$ at time t. Nevertheless it is easier to keep track of the total outcome at all no trap nodes $\sum_{k\neq 1}\pi_{\boldsymbol{k}\boldsymbol{j}}(t)$. The complete orthonormal basis set $\sum_{k\neq 1}|\boldsymbol{k}\rangle\langle\boldsymbol{k}| = \mathbf{1} - |\mathbf{1}\rangle\langle\mathbf{1}|$ leads to, see [1],

$$\sum_{k\neq 1}\pi_{\boldsymbol{k},\boldsymbol{j}}(t) = \sum_{l=1}^{N} \mathrm{e}^{-2\gamma_l t}\langle\boldsymbol{j}|\boldsymbol{\Phi}_l\rangle\langle\tilde{\boldsymbol{\Phi}}_l|\boldsymbol{j}\rangle - \sum_{l,l'=1}^{N} \mathrm{e}^{-\mathrm{i}(\lambda_l-\lambda_{l'}^*)}\langle\boldsymbol{j}|\boldsymbol{\Phi}_{l'}\rangle\langle\tilde{\boldsymbol{\Phi}}_{l'}|\mathbf{1}\rangle\langle\mathbf{1}|\boldsymbol{\Phi}_l\rangle\langle\tilde{\boldsymbol{\Phi}}_l|\boldsymbol{j}\rangle. \tag{17}$$

Thus the mean survival probability looks like

$$\Pi_M(t) = \frac{1}{N-1}\sum_{l=1}^{N} \mathrm{e}^{-2\gamma_l t}[1-2\langle\tilde{\boldsymbol{\Phi}}_l|\mathbf{1}\rangle\langle\mathbf{1}|\boldsymbol{\Phi}_l\rangle] + \frac{1}{N-1}\sum_{l,l'=1}^{N} \mathrm{e}^{-\mathrm{i}(\lambda_l-\lambda_{l'}^*)t}[\langle\tilde{\boldsymbol{\Phi}}_{l'}|\mathbf{1}\rangle\langle\mathbf{1}|\boldsymbol{\Phi}_l\rangle]^2. \tag{18}$$

Increasing the fractal generation g, the ratio $1/N$ becomes very small, which makes $2\langle\tilde{\boldsymbol{\Phi}}_l|\mathbf{1}\rangle\langle\mathbf{1}|\boldsymbol{\Phi}_l\rangle \ll 1$, and at long time the oscillating term of equation (18) vanishes. Thus $\Pi_M(t)$ is reduced to

$$\Pi_M(t) \approx \frac{1}{N-1}\sum_{l=1}^{N}\exp(-2\gamma_l t). \tag{19}$$

If the smallest $\gamma_l = \gamma_{\min}$ is much smaller than the others, then for $t \gg 1/\gamma_{\min}$, $\Pi_M(t) = \exp(-2\gamma_{\min}t)$ as shown in [27]. Figure 5 shows the behaviour of $\Pi_M(t)$ versus time in double logarithmic scale for different trap strengths for RHFs of generation $g = 3$ for functionality $f = 3$ (a) and $f = 4$ (b). At short times all curves assume values close to 0 (probability close to 1). For large t we find a plateau larger than 0 for the presence of real eigenvalues, see also [32]. In fact there are $(3^g-1)/2+(f+1)^g-3^g$ real degenerate eigenvalues, see [20], for which $\gamma_l = 0$ holds. Therefore one can rewrite equation (19) as

$$\Pi_M(t) = \frac{1}{N-1}\left[(3^g-1)/2+(f+1)^g-3^g+\sum_{\gamma_l\neq 0}\exp(-2\gamma_l t)\right]. \tag{20}$$

Equation (20) for $t \to \infty$ reads

$$\lim_{t\to\infty}\Pi_M(t) = \frac{1}{N-1}[(3^g-1)/2+(f+1)^g-3^g]. \tag{21}$$

At intermediate time range, there are interesting counterintuitive features of the curves; in fact, one could think that fast decreases of $\Pi_m(t)$ correspond to big values of γ. In contrast for

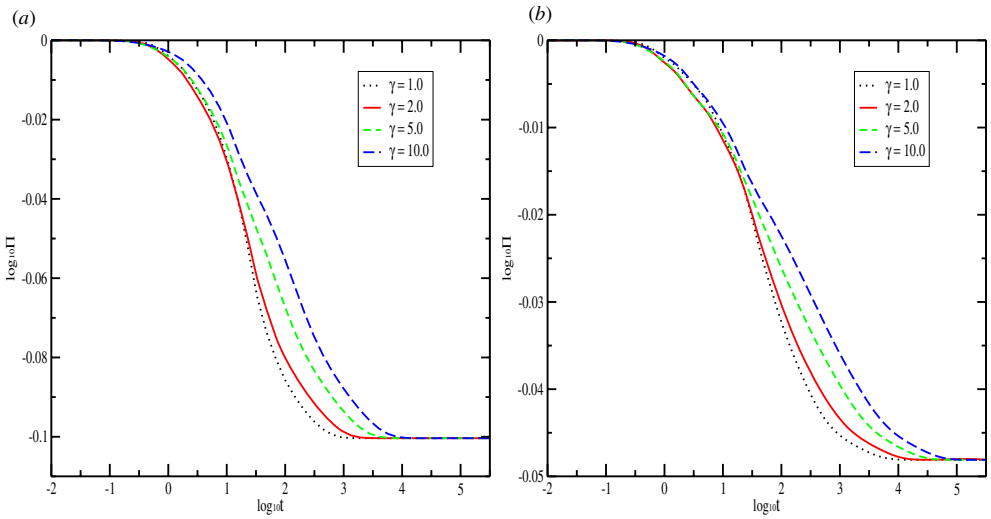

Figure 5. Mean survival probability of RHFs of generation $g = 3$ for functionality $f = 3$ (a) and functionality $f = 4$ (b).

deep traps, $\gamma = 10$ for instance, the probability decreases later to the plateau. We could also deduce it from figure 3 because there are $(3^g - 1)/2$ (number of non-degenerate eigenvalues save λ_{purple}, see also equation (23) of [20]) complex eigenvalues with small positive γ_l and thus its corresponding exponential terms of equation (20) vanish at late time.

6. Can CTQWs be useful for plant photosynthesis?

In plant physiology we have two basic questions to answer at different scales: how much can a plant photosynthesize? How can we measure it? Special complexes inside the leaf harvest energy from the incoming sunlight radiation and transport it very quickly through the lattice to special sites, the reactive centres, where the Calvin cycle fixes the atmospheric carbon. Actually many of the existing and accepted models are based on the theory developed by Farquhar *et al* [33] and obtain some fundamental parameters like the electron transfer rate from experiments but not from a robust quantum theory. The carbon uptake is of course a very complicated task to forecast because it involves a lot of different variables and environmental boundary conditions, but CTQWs could help to understand aspects of the light-dependent reactions of photosynthesis. Moreover, an open issue for the community is to determine how to connect the so-called SIF (solar induced fluorescence) outcoming from plants (a portion of the untrapped energy) with the carbon uptake (related to the energy entered into the reactive centres) [34, 35]. It is then important to know the ratio between the trapped and the untrapped energy and in this framework CTQWs can result useful.

7. Conclusion

In summary, in this work we focused on the eigenvalue spectrum of regular hyperbranched fractals of general functionality f with central trap. The first goal is that the degenerate eigenvalues are real, independent from the trap strength and analytically calculable. These

real eigenvalues bring to the final plateau of the mean survival probability larger than zero. The imaginary eigenvalues are non-degenerate and for deep traps just one has a big imaginary part while the imaginary part of the others tends to zero. This fact causes the delay to attain the final plateau of the mean survival probability. It was also discovered and demonstrated only for $g = 1$ that for infinitely deep traps, just one eigenvalue is imaginary while the others are real and appear with occurrence multiple of f. Finally we noted that: (a) the network symmetries, which determine the degeneracy of the eigenvalues, influence the final probability of being outside the trap. (b) The perturbative parameter γ modifies the rate of the harvesting process. Hence the perturbed quantum walks might be a good tool to study the kinetics of the light-dependent reactions in plant photosynthesis.

Acknowledgments

I would like to thank Professor Blumen and Dr Mülken for the fruitful discussions. This work was supported by a grant from the Ministry of Science, Research and the Arts of Baden-Württemberg (AZ: 24-7532.23-11-11/1). Further support from the Deutsche Forschungsgemeinschaft (DFG) and the Fonds der Chemischen Industrie is gratefully acknowledged.

References

[1] Mülken O, Blumen A, Amthor T, Giese C, Reetz-Lamour M and Weidemüller M 2007 *Phys. Rev. Lett.* **99** 090601
[2] Mülken O and Blumen A 2008 arXiv:0810.4052v1
[3] Fleming G R and Scholes G D 2004 *Nature* **431** 256
[4] Cheng Y C and Silbey R 2006 *Phys. Rev. Lett.* **96** 028103
[5] Engel G S, Calhoun T R, Read R L, Ahn T, Manal T, Cheng Y C, Blankenship R and Fleming G R 2007 *Nature* **446** 782
[6] Aharonov Y, Davidovich L and Zagury N 1993 *Phys. Rev.* A **48** 1687
[7] Farhi E and Gutmann S 1998 *Phys. Rev.* A **58** 915
[8] Kempe J 2003 *Contemp. Phys.* **44** 307
[9] Blumen A, Volta A, Jurjiu A and Koslowski Th 2005 *Physica* A **356** 12
[10] Weiss G H 1994 *Aspects and Applications of the Random Walk* (Amsterdam: North-Holland)
[11] van Kampen N 1990 *Stochastic Processes in Physics and Chemistry* (Amsterdam: North-Holland)
[12] Gorenflo R, Mainardi F and Vivoli A 2007 *Chaos Solitons Fractals* **34** 87
[13] Blumen A, Jurjiu A, Koslowski Th and von Ferber C 2003 *Phys. Rev.* E **67** 061103
[14] Jafarizadeh M A, Sufiani R, Salimi S and Jafarizadeh S 2007 *Eur. Phys. J.* B **59** 199
[15] Childs A M and Goldstone J 2004 *Phys. Rev.* A **70** 022314
[16] Mülken O and Blumen A 2005 *Phys. Rev.* E **71** 016101
[17] Thurner S and Tsallis C 2005 *Europhys. Lett.* **72** 197
[18] Volta A, Mülken O and Blumen A 2006 *J. Phys. A: Math. Gen.* **39** 14997
[19] Jayanthy C S and Wu S Y 1993 *Phys. Rev.* B **48** 10188
[20] Blumen A, von Ferber C, Jurjiu A and Koslowski Th 2004 *Macromolecules* **37** 638
[21] Galiceanu M and Blumen A 2007 *J. Chem. Phys.* **127** 134902
[22] Mülken O, Bierbaum V and Blumen A 2006 *J. Chem. Phys.* **124** 124905
[23] Xu X P and Liu F 2008 *Phys. Lett.* A **372** 6727
[24] Cullum J K and Willoughby R 1985 *Lanczos Algorithms for Large Symmetric Eigenvalue Problems, vol. I: Theory, vol. II: Programs* (Boston: Birkäuser)
[25] Sakurai J 1994 *Modern Quantum Mechanics* 2nd edn (Redwood City, CA: Addison-Wesley)
[26] Pearlstein R M 1972 *J. Chem. Phys.* **56** 2431
[27] Parris P E 1989 *Phys. Rev.* B **40** 4928
[28] Horn R A and Johnson C R 1985 *Matrix Analysis* (Cambridge: Cambridge University Press)
[29] Smith B T, Boyle J M, Garbow B S, Ikebe Y, Klema V C and Moler C B 1976 *Matrix Eigensystem Routines—EISPACK Guide (Lecture Notes in Computer Science* vol 6*)* (Berlin: Springer)

[30] Bar-On I and Ryaboy V 1997 *J. Sci. Comput.* **18** 1412
[31] Scott N H 1993 *Proc. R. Soc. Lond.* A **441** 625
[32] Agliari E, Mülken O and Blumen A 2009 arXiv:0903.3288v1
[33] Farquhar G, von Caemmerer S and Berry J 1980 *Planta* **149** 78
[34] van der Tol C, Verhoef W and Rosema A 2009 *Agric. Forest Meteorol.* **149** 96
[35] Miglietta F, Gioli B, Toscano P, Magnani F and Volta A 2009 in preparation